SCIENTIFIC RESEARCH

# COMPARATIVE ASSESSMENT OF EXPIRATORY GROUND-GLASS LESION CHANGES ACROSS PULMONARY DISEASE SUBTYPES ON QUANTITATIVE CT AT NGOC MINH CLINIC, VIETNAM

***Hoang Thi Trieu Nghi*, Bui Nguyen Canh**, Cao Xuan Minh*, Nguyen Thanh Luu*, Bui Chien Thang***, Tran Van Ngoc****

**SUMMARY**

**Background:** Quantitative computed tomography (QCT) enables sensitive evaluation of dynamic parenchymal changes in lung disease, yet the behavior of expiratory ground-glass (GG) lesion change across different pulmonary phenotypes remains insufficiently characterized.

**Objective:** To compare inspiratory–expiratory GG change across dominant QCT-defined pulmonary groups.

**Methods:** This retrospective study included 46 patients who underwent paired inspiratory–expiratory QCT at Ngoc Minh Clinic. GG lesion percentages were extracted separately for the right and left lungs. GG change (%) was calculated as the relative difference between expiratory and inspiratory GG values. Patients were categorized into air trapping, emphysema, interstitial lung disease (ILD), and normal groups based on dominant QCT findings. Between-group differences were assessed using non-parametric tests, and within-subject lung-side differences were evaluated using linear mixed-effects modeling.

**Results:** GG change differed significantly among disease groups in both lungs ($p < 0.001$). The air trapping group demonstrated markedly higher GG change compared with emphysema, ILD, and normal lungs (all $p < 0.05$). No significant difference in GG change was observed between the right and left lungs, and no lung-side–by–group interaction was identified.

**Conclusion:** Expiratory GG change effectively distinguishes air trapping from other pulmonary phenotypes and represents a symmetric functional QCT marker of small airway dysfunction.

***Keywords:*** *Quantitative computed tomography, Ground-glass opacity, Air trapping, Expiratory C, Small airway disease*

** Ngoc Minh Clinic*

*** United Imaging Healthcare Vietnam*

**** IDS Medical Systems Vietnam Co.,Ltd*

## I. INTRODUCTION

Quantitative Computed Tomography (QCT) has become an essential non-invasive tool in the phenotyping and monitoring of various chronic lung diseases, including Chronic Obstructive Pulmonary Disease (COPD), interstitial lung disease (ILD), and small airway disease. Traditional inspiratory-phase CT imaging provides important structural information, but it may fail to capture dynamic changes associated with air trapping and ventilation heterogeneity, especially in early disease stages or mild cases without overt structural destruction [1]with the goal of contributing to a personalized approach to the treatment of patients with COPD. Quantitative CT is useful for identifying and sequentially evaluating the extent of emphysematous lung destruction, changes in airway walls, and expiratory air trapping. However, visual assessment of CT scans remains important to describe patterns of altered lung structure in COPD. The classification system proposed and illustrated in this article provides a structured approach to visual and quantitative assessment of COPD. Emphysema is classified as centrilobular (subclassified as trace, mild, moderate, confluent, and advanced destructive emphysema [2].

Expiratory CT, when paired with inspiratory imaging, can highlight functional impairments such as air trapping and expiratory ground-glass opacities—features that often correspond to small airway obstruction, bronchiolar collapse, or ventilation inhomogeneity [3] [4]. The assessment of ground-glass (GG) lesions has historically been qualitative or semi-quantitative; however, recent advances in QCT now allow automated, volumetric quantification of parenchymal patterns across both respiratory phases [5] [6].

Despite growing interest in expiratory imaging, systematic comparisons of ground-glass (GG) behavior across pulmonary disease subtypes remain limited. In particular, how GG attenuation patterns change from inspiration to expiration among patients with air trapping, emphysema, interstitial lung disease, and normal lungs is not fully understood. Quantitative assessment of dynamic GG change using paired inspiratory–expiratory QCT provides an objective marker of small airway dysfunction that may be missed on conventional inspiratory CT alone. This approach can facilitate early detection of air trapping in patients with inconclusive spirometry or minimal visual abnormalities, support functional phenotyping of diffuse lung diseases, and improve differentiation between airway-predominant and parenchymal-predominant processes, thereby enhancing the clinical interpretation of functional lung imaging.

This study therefore aims to quantify the percentage change in GG lesions between inspiratory and expiratory CT scans across multiple disease groups and to determine whether such changes can be used to differentiate disease phenotypes.

## II. SUBJECTS AND METHODS

### 1. **Study Population**

This retrospective study included 46 adult patients (mean age: 59.8 ± 12.7 years; 61% male) who underwent clinically indicated paired inspiratory and expiratory chest CT scans between March and April 2025 at Ngoc Minh Clinic in Ho Chi Minh City, Vietnam. Patients were categorized into four groups based on consensus interpretation by thoracic radiologists and dominant QCT findings: (1) *Air Trapping* +, (2) *Emphysema*, (3) *Interstitial Lung Disease (ILD)* including both fibrotic and non-fibrotic subtypes, and (4) *Normal* lung parenchyma. Patients with incomplete data or artifacts significantly affecting lung segmentation were excluded.

### 2. CT Protocol and Image Analysis

All scans were performed using a standardized inspiratory-expiratory CT protocol on a 128-slice multidetector scanner (Revolution EVO, GE Healthcare). Images were acquired at full inspiration (TLC) and end expiration (RV), reconstructed with 0.625-1.25-mm slice thickness, and analyzed using a validated CT software platform (Thoracic VCar, GE Healthcare) [7].

Ground-glass (GG) lesions were defined as regions with attenuation values between –703 and –368 HU without obscuration of underlying vessels [8]comparing the consistency of tools. Materials and Methods: Included in the study group were 120 COVID-19 patients (56 women and 104 men; 61 years of median age; range: 21–93

years. Automated segmentation and quantification of GG lesion volumes were performed for each lung separately in both respiratory phases. The percentage change in ground-glass lesion volume was calculated using the following formula:

$$\text{GG Change (\%)} = \frac{(\text{Expiratory GG} - \text{Inspiratory GG})}{\text{Inspiratory GG}} \times 100$$

Definition of dominant QCT patterns

Dominant QCT patterns were defined based on combined visual assessment of paired inspiratory–expiratory CT images and quantitative findings.

+ Normal lungs were defined as the absence of significant parenchymal abnormalities on both inspiratory and expiratory CT, including no evidence of air trapping, emphysema, or interstitial disease. Representative imaging examples are shown in Appendix 1.
+ Air trapping was defined as areas of persistently low attenuation on expiratory CT with relative attenuation normalization on inspiratory images, in the absence of dominant emphysematous destruction or interstitial abnormalities. Cases were classified as air trapping when this finding represented the predominant abnormality. An example of illustrative imaging is presented in Appendix 2.

+ Emphysema was defined by the presence of low-attenuation areas on inspiratory CT consistent with parenchymal destruction and reduced vascular markings. To minimize confounding, cases with emphysematous changes associated with clinically diagnosed asthma were excluded based on information provided by respiratory physicians, including clinical history and pulmonary function testing. An imaging example is provided in Appendix 3.

+ Interstitial lung disease (ILD) was defined by the presence of diffuse parenchymal abnormalities on inspiratory CT, including reticulation, ground-glass opacities with architectural distortion, traction bronchiectasis, or honeycombing, and included both fibrotic and non-fibrotic subtypes. When ILD features coexisted with other abnormalities, ILD was considered the dominant pattern. An example is shown in Appendix 4.

Each case was assigned to a single dominant QCT group based on the predominant imaging pattern to allow mutually exclusive classification for statistical analysis.

**3. Statistical Analysis**

Descriptive statistics were used to summarize demographic and clinical characteristics. Continuous variables are presented as median values with distribution ranges. For descriptive purposes, GG change distributions within each disease group and lung side were summarized using the median and a 95% distribution interval defined as mean ± 2 standard deviations (SD), reflecting the biological variability of GG change rather than the confidence interval of the median.

Between-group comparisons of GG change were performed separately for the right and left lungs using the Kruskal–Wallis test. When the overall test was significant, pairwise comparisons were conducted using the Mann–Whitney U test, with p values reported for key clinically relevant comparisons.

To assess within-subject differences between the right and left lungs and to account for the paired structure of the data, a linear mixed-effects model (LMM) was constructed. GG change was modeled as the dependent variable, with lung side (right vs left), disease group, and their interaction included as fixed effects, and subject identity included as a random effect. An extended model incorporating a random slope for lung side was also evaluated to allow subject-specific asymmetry.

All statistical tests were two-sided, and a p value < 0.05 was considered statistically significant. Statistical analyses were performed using Python (version 3.11.2, SciPy and stats models libraries) by Dr. HTTN.

## III. RESULTS

A total of 46 patients were included in the analysis (28 men, 18 women; age range: 40–84 years). Patients were classified according to the dominant QCT pattern determined by expert interpretation, 17 patients were categorized as *Air Trapping* +, 14 as *Emphysema*, 8 as

*ILD* (non-fibrotic: n=6, fibrotic: n=2), and 7 as *Normal*. The average inspiratory-to-expiratory change in ground-glass (GG) lesions was significantly higher in the *Air Trapping* + group compared to all other groups. Representative HRCT images, quantitative measurements, and examples illustrating GG change calculations across the four groups are presented in Appendices 1 through 4.

For the right lung, the median GG change and 95% CI (mean ± 2SD) for each group were:

**Table 1. GG Change on the right lung**

| Group | N | Median (%) | 95% CI lower | 95% CI upper |
|---|---|---|---|---|
| Air trapping | 13 | 337.9 | 52.7 | 552.2 |
| Emphysema | 11 | 31.2 | −84.0 | 195.4 |
| ILD | 8 | 143.5 | −136.1 | 459.9 |
| Normal | 8 | 117.3 | −73.2 | 346.4 |

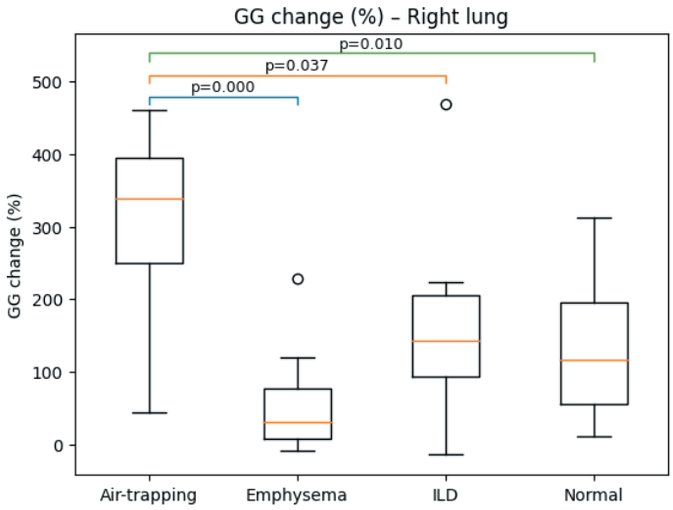


**Figure 1. GG change on Right Lung by Disease group.** The comparisons are shown (Mann–Whitney U): Air trapping vs Emphysema ($p < 0.001$), Air trapping vs ILD ($p = 0.037$), Air trapping vs Normal ($p = 0.010$).

For the left lung, the median GG change and 95% CI (mean ± 2SD) for each group were:

**Table 1. GG Change on the left lung**

| Group | N | Median (%) | 95% CI lower | 95% CI upper |
|---|---|---|---|---|
| Air trapping | 13 | 320.3 | 20.6 | 612.0 |
| Emphysema | 11 | 33.7 | −81.9 | 207.2 |
| ILD | 9 | 131.1 | −149.3 | 446.6 |
| Normal | 8 | 122.3 | −72.0 | 365.7 |

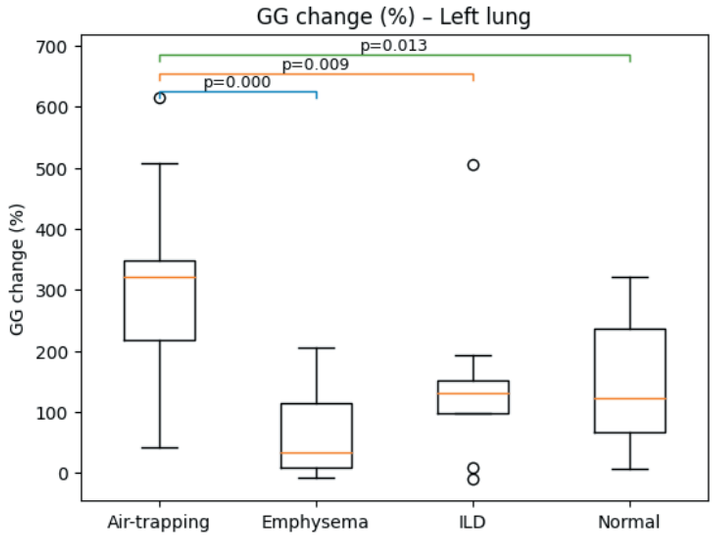


**Figure 2. GG change on Left Lung by Disease group.** The comparisons are shown (Mann–Whitney U): Air trapping vs Emphysema ($p < 0.001$), Air trapping vs ILD ($p = 0.009$), Air trapping vs Normal ($p = 0.013$).

Boxplots of ground-glass opacity (GG) change (%) across dominant QCT groups in the right (table 1 & figure 1) and left (table 2 & figure 2) lungs. GG change was significantly higher in the air trapping group compared with emphysema, interstitial lung disease (ILD), and normal lungs in both lungs. P values were calculated using the Mann–Whitney U test.

Median GG change was highest in the air trapping group in both lungs (right: 337.9%, left: 320.3%), with wide but upward-shifted 95% distribution intervals (mean ± 2SD). In contrast, emphysema showed minimal GG change with intervals overlapping zero, whereas ILD and normal lungs demonstrated intermediate values with substantial overlap.

### Side-Specific Effects

Ground-glass opacity (GG) change differed significantly among dominant QCT groups in both lungs (right lung: Kruskal–Wallis $H = 17.21$, $p = 0.0006$; left lung: $H = 17.79$, $p = 0.0005$). Patients with air trapping demonstrated markedly higher GG change compared with other groups. Post-hoc analysis revealed a significant difference between the air trapping and emphysema groups in both the right and left lungs (Bonferroni-adjusted $p = 0.0025$ for both), whereas differences between other group pairs were not statistically significant. No significant difference in GG change was observed between the right and left lungs, either in the overall cohort or within individual QCT groups (all $p > 0.3$) after accounting for within-subject correlation using a mixed-effects model, indicating symmetric behavior of GG change across lungs.

## IV. DISCUSSION

This study demonstrates that the expiratory behavior of ground-glass lesions varies significantly across common pulmonary disease subtypes, as assessed by quantitative CT. The most striking finding was the markedly elevated percentage increase in GG lesions during expiration in patients with *Air Trapping* +, supporting the hypothesis that such patients exhibit significant small airway dysfunction that is only revealed during forced expiration.

The use of paired inspiratory–expiratory QCT allowed for functional imaging that goes beyond structural assessment. In diseases such as COPD and bronchiolitis, air trapping leads to hyperinflation and dynamic changes that are otherwise invisible on standard inspiratory CT [1,2]. Our results align with prior work suggesting that expiratory GG opacities may represent gas retention within partially collapsed or poorly ventilated alveoli [3]. Within the asthma–COPD overlap spectrum, structural abnormalities such as airway wall thickening and lobular air trapping are frequently observed [9]. Quantitative

CT (QCT) offers objective measures of small-airway dysfunction—such as the expiratory-to-inspiratory mean lung density ratio (E/I-MLD) and expiratory–inspiratory relative volume changes across HU thresholds using parametric response mapping for functional small airways disease (PRM-fSAD). These metrics correlate with airflow obstruction severity and enable more refined disease phenotyping beyond visual CT assessment [10].

Interestingly, patients with *ILD*—regardless of fibrosis-showed moderate changes in GG percentage but not significantly different from those with *Normal* lungs. This may reflect the mixed restrictive pattern of ILD, where small airway obstruction is not the primary mechanism. The *Emphysema* group demonstrated limited GG change, likely due to reduced parenchymal tissue available to express such changes.

Finally, our findings indicate that GG change varies primarily according to disease phenotype rather than lung side. The consistently higher GG change observed in the air trapping group supports its role as a dynamic marker of small airway dysfunction. The absence of significant right–left differences, even after mixed-effects modeling, suggests that GG change reflects a symmetric global ventilation abnormality, reinforcing its robustness for cross-group comparisons without the need for side-specific adjustment.

**Limitations**

Our study has several limitations. The sample size, though adequate for initial statistical exploration, may limit generalizability. We used automated segmentation tools, which, while validated, may have small inaccuracies in diseased lungs. Furthermore, the mixed disease phenotypes in some patients could blur distinctions between groups. Prospective studies with standardized acquisition protocols and larger cohorts are warranted.

## V. CONCLUSION

Quantitative expiratory GG lesion changes provide important insights into functional differences between lung disease subtypes. *Air Trapping* + patients exhibit the most pronounced changes, affirming the role of expiratory CT in revealing small airway pathology. The consistent symmetry between lungs also points to the need for side-specific assessment in QCT analysis.

**Acknowledgements**

The authors would like to thank the Department of Radiology and Pulmonology at Ngoc Minh Clinic, especially Assoc. Prof. Ngoc Tran Van, for their support in providing access to the CT imaging database and clinical annotations. We also acknowledge the technical assistance from the QCT analysis team for ensuring data quality and consistency.

## REFERENCES

1. D. A. Lynch *et al.*, “CT-Definable Subtypes of Chronic Obstructive Pulmonary Disease: A Statement of the Fleischner Society.,” *Radiology*, vol. 277, no. 1, pp. 192–205, Oct. 2015, doi: 10.1148/radiol.2015141579.
2. H. Arakawa and W. R. Webb, “Air trapping on expiratory high-resolution CT scans in the absence of inspiratory scan abnormalities: correlation with pulmonary function tests and differential diagnosis.,” *AJR Am J Roentgenol*, vol. 170, no. 5, pp. 1349–1353, May 1998, doi: 10.2214/ajr.170.5.9574614.
3. A. Madani, J. Zanen, V. de Maertelaer, and P. A. Gevenois, “Pulmonary emphysema: objective quantification at multi-detector row CT--comparison with macroscopic and microscopic morphometry.,” *Radiology*, vol. 238, no. 3, pp. 1036–1043, Mar. 2006, doi: 10.1148/radiol.2382042196.
4. D. A. Lynch, “Functional imaging of COPD by CT and MRI.,” *Br J Radiol*, vol. 95, no. 1132, p. 20201005, Apr. 2022, doi: 10.1259/bjr.20201005.
5. “Galbán, C., Han, M., Boes, J. et al. Computed tomography–based biomarker provides unique signature for diagnosis of COPD phenotypes and disease progression. Nat Med 18, 1711–1715 (2012). https://doi.org/10.1038/nm.2971”.

6. C. R. Kliment *et al.*, “A comparison of visual and quantitative methods to identify interstitial lung abnormalities.,” *BMC Pulm Med*, vol. 15, p. 134, Oct. 2015, doi: 10.1186/s12890-015-0124-x.

7. “U.S. FDA. 510(k) Premarket Notification—THORACIC VCAR (K103480). (FDA 510(k) PDF).” [Online]. Available: https://www.accessdata.fda.gov/cdrh_docs/pdf10/K103480.pdf

8. V. Granata *et al.*, “Quantitative Analysis of Residual COVID-19 Lung CT Features: Consistency among Two Commercial Software,” *Journal of Personalized Medicine*, vol. 11, no. 11, 2021, doi: 10.3390/jpm11111103.

9. D. Lu, H. Yu, L. Chen, J. Lin, S. Chen, and Y. Huang, “Differences in the Quantitative HRCT Characteristics of Patients with Asthma, COPD and Asthma-COPD Overlap and Their Relationships with Pulmonary Function.,” *Int J Chron Obstruct Pulmon Dis*, vol. 19, pp. 1775–1789, 2024, doi: 10.2147/COPD.S469956.

10. T.-N. Hoang-Thi, G. Chassagnon, T. Hua-Huy, V. Boussaud, A.-T. Dinh-Xuan, and M.-P. Revel, “Chronic Lung Allograft Dysfunction Post Lung Transplantation: A Review of Computed Tomography Quantitative Methods for Detection and Follow-Up.,” *J Clin Med*, vol. 10, no. 8, Apr. 2021, doi: 10.3390/jcm10081608.

Correspondent: Hoang Thi Trieu Nghi. Email: hoang.thi.trieu.nghi@gmail.com

Received: 16/07/2025. Assessed: 25/07/2025. Accepted: 10/12/2025

**Appendix 1:** Quantitative HRCT in the coronal plane of a 46-year-old normal male patient. Coronal inspiration CT (A,B), the correspondent lung composition statistic table (C); Coronal expiration CT (D,E), the correspondent lung composition statistic table (F). Lung parenchyma within the ground-glass attenuation (highlighted in pink) range accounts for 8% of the right lung and 9.6% of the left lung on the inspiratory phase (A,B), showing a mild increase on expiration to 16.5% in the right lung and 21.5% in the left lung (D,E). The parenchyma falling within the ground-glass attenuation threshold is predominantly distributed in the lung bases, which may be attributable to gravitational effects. The percentage change in ground-glass opacities is calculated as (16.5 − 8)/8 = 106% for the right lung and (21.5 − 9.6)/9.6 = 124% for the left lung.

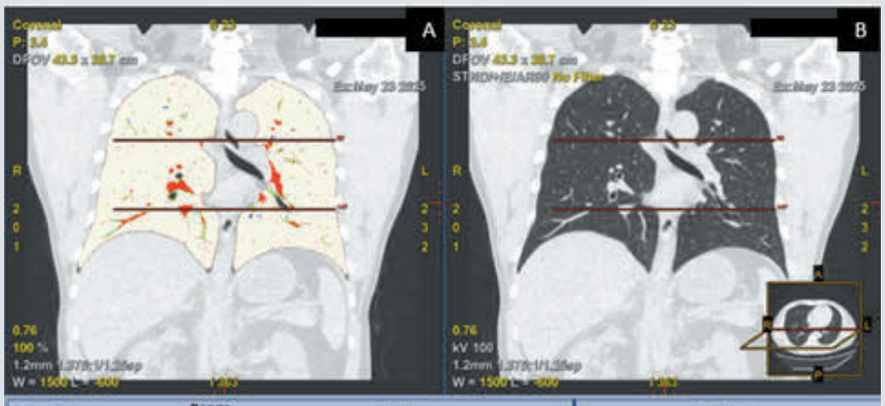


C

| Range Name | Range values | Right Lung | Right Lung Upper Zone | Right Lung Middle Zone | Right Lung Lower Zone | Left Lung | Left Lung Upper Zone | Left Lung Middle Zone | Left Lung Lower Zone |
|---|---|---|---|---|---|---|---|---|---|
| Emphysema | [-1024 / -977[ | 0.1208 % | 0.1197 % | 0.1429 % | 0.0824 % | 0.1471 % | 0.084 % | 0.1577 % | 0.1724 % |
| Pulmonary Parenchyma | [-977 / -703[ | 88.9916 % | 90.7844 % | 89.2328 % | 87.0986 % | 87.2646 % | 89.8732 % | 87.6035 % | 85.225 % |
| Ground Grass Opacity | [-703 / -368[ | 8.0099 % | 7.3234 % | 6.9784 % | 10.4145 % | 9.602 % | 8.248 % | 8.322 % | 12.0687 % |
| Other | [-368 / -100[ | 1.6695 % | 1.2046 % | 1.8986 % | 1.6388 % | 1.8737 % | 1.2716 % | 2.1854 % | 1.8472 % |
| Consolidation | [-100 / 100[ | 1.2082 % | 0.5679 % | 1.7473 % | 0.7657 % | 1.1127 % | 0.5232 % | 1.7315 % | 0.6868 % |
| | Total | 1.8775 L | 0.4247 L | 0.9319 L | 0.521 L | 1.4757 L | 0.3145 L | 0.6508 L | 0.5103 L |

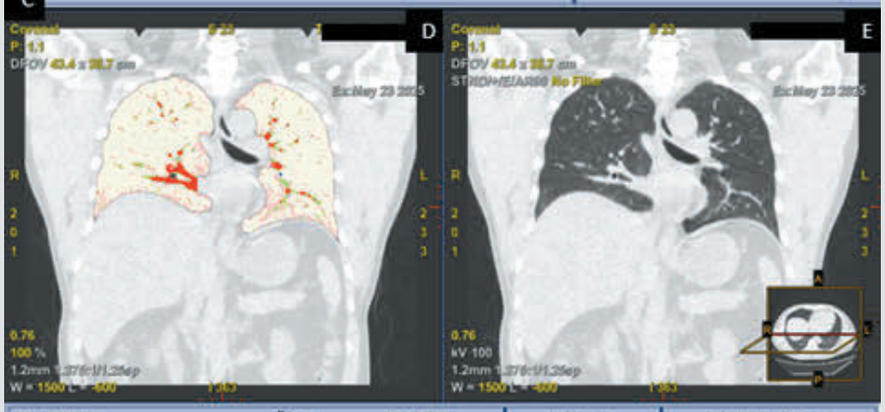


F

| Range Name | Range values | Right Lung | Left Lung | Total Lung Volume |
|---|---|---|---|---|
| | | Right Lung | Left Lung | Combined Lungs |
| Emphysema | [-1024 / -977[ | 0.1134 % | 0.0726 % | 0.0956 % / 0.0023 L |
| Pulmonary Parenchyma | [-977 / -703[ | 79.4537 % | 74.1849 % | 77.1551 % / 1.8814 L |
| Ground Grass Opacity | [-703 / -368[ | 16.5965 % | 21.5171 % | 18.7432 % / 0.457 L |
| Other | [-368 / -100[ | 2.3763 % | 2.8049 % | 2.5633 % / 0.0625 L |
| Consolidation | [-100 / 100[ | 1.4602 % | 1.4204 % | 1.4428 % / 0.0352 L |
| | Total | 1.3746 L | 1.0638 L | 2.4385 L |

**Appendix 2:** Example of Air trapping lung in bipasic CT of a 67-year-old male patient. Coronal inspiration CT (A,B), the correspondent lung composition statistic table (C); Coronal expiration CT (D,E), the correspondent lung composition statistic table (F). On the inspiratory phase, only minimal ground-glass opacities are present, highlighted in pink (A, B). The ground-glass regions are more clearly visualized on the expiratory phase, appearing as air trapping pattern (D,E). Quantitative analysis demonstrates that ground-glass opacities account for 6.8% of the right lung parenchyma and 6.2% of the left lung on inspiration and increase markedly to 29.95% of the right lung and 28.2% of the left lung on expiration. The percentage change in ground-glass opacities is calculated as (29.95 – 6.8)/6.8 = 340% for the right lung and (28.2 – 6.2)/6.2 = 354% for the left lung.

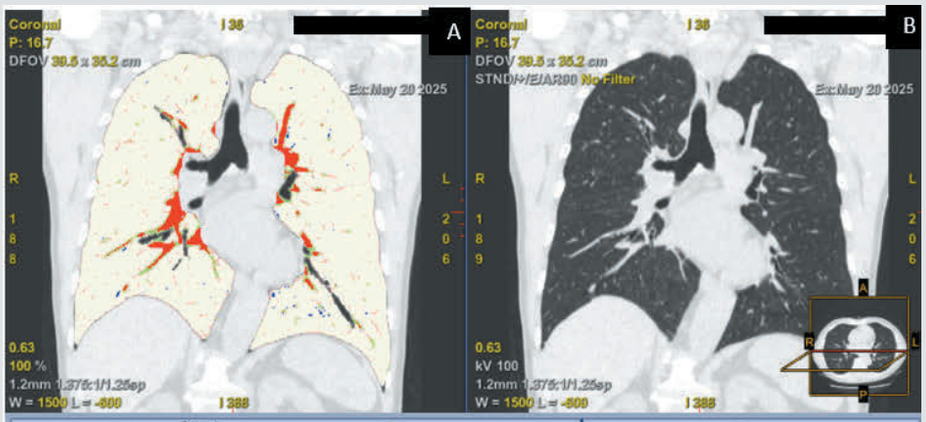


C

| Range Name | Range values | Right Lung | Right Lung | Right Lung | Right Lung | Left Lung | Left Lung | Left Lung | Left Lung |
|---|---|---|---|---|---|---|---|---|---|
| | | Right Lung | Upper Zone | Middle Zone | Lower Zone | Left Lung | Upper Zone | Middle Zone | Lower Zone |
| Emphysema | [-1024 / -977[ | 0.1809 % | 0.1268 % | 0.1636 % | 0.2389 % | 0.4387 % | 0.36 % | 0.2872 % | 0.6359 % |
| Pulmonary Parenchyma | [-977 / -703[ | 90.2865 % | 92.1289 % | 89.4989 % | 90.1194 % | 90.7313 % | 92.3916 % | 90.0326 % | 90.5467 % |
| Ground Grass Opacity | [-703 / -368[ | 6.8397 % | 6.1158 % | 6.7169 % | 7.474 % | 6.2289 % | 5.8346 % | 5.8218 % | 6.858 % |
| Other | [-368 / -100[ | 1.5071 % | 1.0548 % | 1.8205 % | 1.3904 % | 1.444 % | 0.9799 % | 1.8033 % | 1.3282 % |
| Consolidation | [-100 / 100[ | 1.1857 % | 0.5736 % | 1.8001 % | 0.7773 % | 1.1571 % | 0.4339 % | 2.0551 % | 0.6311 % |
| | Total | 2.4674 L | 0.5428 L | 1.0934 L | 0.8312 L | 2.2282 L | 0.4704 L | 0.8881 L | 0.8696 L |

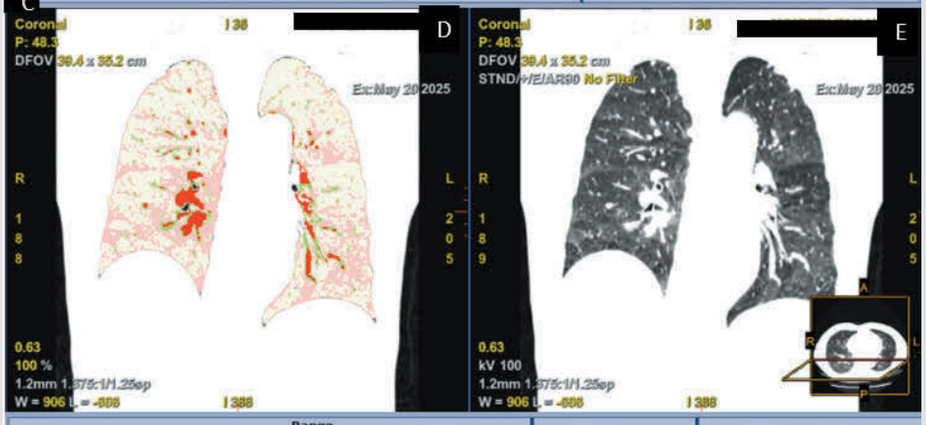


F

| Range Name | Range values | Right Lung | Left Lung | Total Lung Volume |
|---|---|---|---|---|
| | | Right Lung | Left Lung | Combined Lungs |
| Emphysema | [-1024 / -977[ | 0.0178 % | 0.059 % | 0.037 % / 0.0009 L |
| Pulmonary Parenchyma | [-977 / -703[ | 64.1317 % | 68.3448 % | 66.0892 % / 1.59 L |
| Ground Grass Opacity | [-703 / -368[ | 29.9527 % | 26.1825 % | 28.201 % / 0.6785 L |
| Other | [-368 / -100[ | 3.6149 % | 3.4817 % | 3.553 % / 0.0855 L |
| Consolidation | [-100 / 100[ | 2.2828 % | 1.932 % | 2.1198 % / 0.051 L |
| | Total | 1.288 L | 1.1178 L | 2.4058 L |

**Appendix 3.** Quantitative HRCT in the coronal plane of a 63-year-old male patient diagnosed with COPD. Quantified emphysema, highlighted in blue cyan (A, C), involves 22% of the right lung and 36% of the left lung on inspiration. Quantified ground-glass opacities, highlighted in pink, account for 6% of the right lung parenchyma and 8.2% of the left lung on the inspiratory phase (A,B), with only a minimal increase on expiration to 6.7% in the right lung and 9% in the left lung (C,D). The percentage change in ground-glass opacities is calculated as (6.7 − 6)/6 = 12% for the right lung and (9 − 8.2)/8.2 = 10% for the left lung.

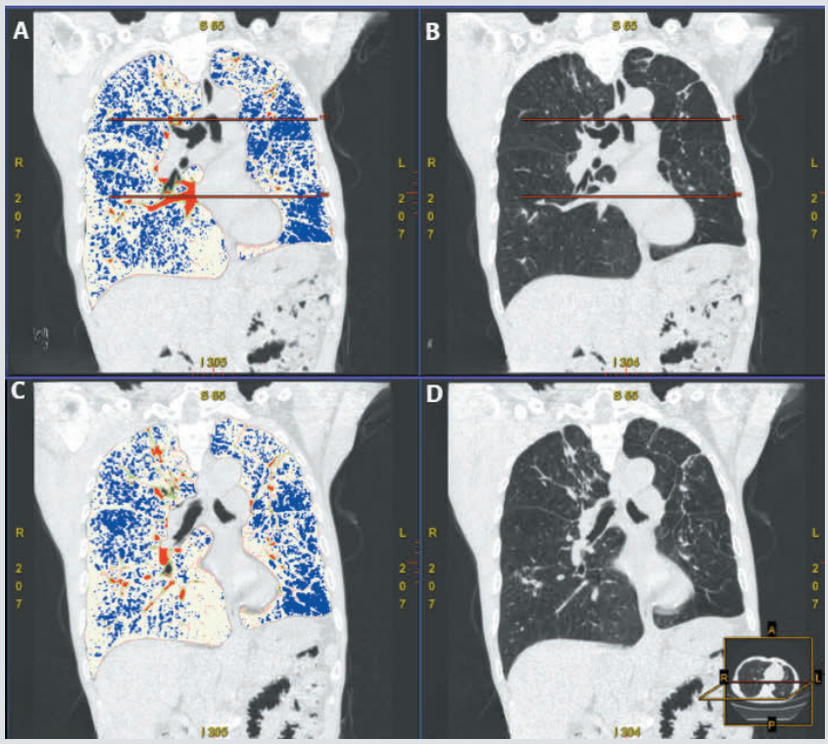


**Appendix 4.** Quantitative HRCT images in the coronal plane of a 55-year-old female patient diagnosed with interstitial lung disease associated with systemic sclerosis. Ground-glass opacities (highlighted in pink) account for 27.4% of the right lung parenchyma and 30% of the left lung parenchyma on the inspiratory phase (A,B), with a slight increase on expiration to 30% in the right lung and 32.3% in the left lung (C,D). The percentage change in ground-glass opacities is calculated as (30 − 27.4)/27.4 = 9% for the right lung and (32.3 − 30)/30 = 8% for the left lung. In addition, the increase in ground-glass opacities on the expiratory phase is predominantly located in the bilateral lung bases.